JACS
JOURNAL OF THE AMERICAN CHEMICAL SOCIETY
Article
pubs.acs.org/JACS

Mixed-Valence Metal Oxide Nanoparticles as Electrochemical Half-Cells: Substituting the Ag/AgCl of Reference Electrodes by CeO_{2-x} Nanoparticles

Rajaram K. Nagarale,[†,§] Udo Hoss,[‡] and Adam Heller*[,§]

[†]Department of Chemical Engineering, Indian Institute of Technology, Kanpur, UP India-208016
[‡]Abbott Diabetes Care, 1360 South Loop Road, Alameda California 94502, United States
[§]McKetta Department of Chemical Engineering, University of Texas, Austin Texas 78712, United States

Supporting Information

ABSTRACT: Cations of mixed valence at surfaces of metal oxide nanoparticles constitute electrochemical half-cells, with potentials intermediate between those of the dissolved cations and those in the solid. When only cations at surfaces of the particles are electrochemically active, the ratio of electrochemically active/all cations is ~0.1 for 15 nm diameter CeO_{2-x} particles. CeO_{2-x} nanoparticle-loaded hydrogel films on printed carbon and on sputtered gold constitute reference electrodes having a redox potential similar to that of Ag/AgCl in physiological (0.14 M) saline solutions. *In vitro* the characteristics of potentially subcutaneously implantable glucose monitoring sensors made with CeO_{2-x} nanoparticle reference electrodes are undistinguishable from those of sensors made with Ag/AgCl reference electrodes. Cerium is 900 times more abundant than silver, and commercially produced CeO_{2-x} nanoparticle solutions are available at prices well below those of the Ag/AgCl pastes used in the annual manufacture of ~10^9 reference electrodes of glucose monitoring strips for diabetes management.

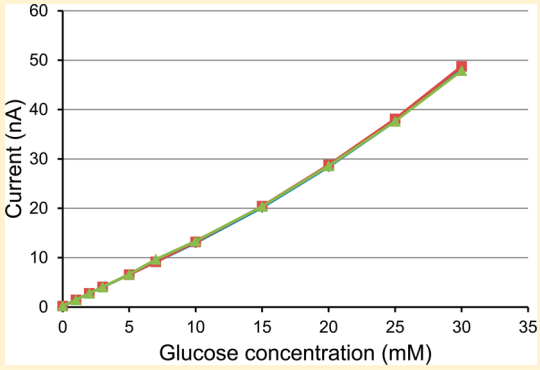

INTRODUCTION

Ag/AgCl is arguably the most widely used electro-active electrode material. It is used in part of the 16 billion[1] annually produced electrochemical single-use strips of glucose monitoring systems for diabetes management, in some as the reference electrode.[2−4] It is also used in subcutaneously implanted sensors of continuously glucose monitoring systems,[5] in pH meters, in blood gas (pO_2 and pCO_2) monitors, and in potentiometric monitors of ion concentrations. In applications where the Ag/AgCl electrode is used for long periods in <1 M Cl^- solutions, depletion of the anion necessitates the use of membranes to reduce the leaching of Cl^-. Furthermore, a 6-fold increase in the price of silver in the past decade raised the cost of Ag and AgCl of glucose assaying strips sufficiently to warrant consideration of their substitution. For ease of their substitution it is necessary that half-cell potential of the alternative electrode be close enough to that of the Ag/AgCl electrode, otherwise owners of existing systems might not be able to continue their use.

Here we expand the family of redox couples to solid mixed-valence metal oxide nanoparticles, showing that their interfacial cations have redox potentials intermediate between those within macroparticles and in the solution phase. As the diameter of the nanoparticles shrinks, the fraction of the interfacial cations increases. The fraction of metal cations residing at the surface of a nanoparticle is $4d_{mo}/d_{np}$ where d_{mo} is the diameter of the metal oxide molecule and d_{np} is the diameter of the nanoparticle. In an exemplary case where d_{mo} = 0.4 nm and d_{np} = 15 nm, about one-tenth of all cations reside at the solution interface and are potentially electroactive.

Cerium is the most abundant lanthanide; its abundance in the earth's crust exceeds 900-fold that of silver.[6] The surface of 10−20 nm CeO_{2-x} nanoparticles comprises Ce^{4+} and Ce^{3+} ions. The nanoparticles are much less oxidizing than the aqueous Ce^{4+}/Ce^{3+} redox couple but far more oxidizing than the mixed-valence CeO_{2-x} macroparticles, which are stable enough to be used in automotive catalytic converters and in self-cleaning ovens. The standard potential of the $Ce_{aq}^{4+} + e^- \leftrightarrow Ce_{aq}^{3+}$ half-cell at 298 °K is +1.72 V, i.e. it is 1.61 V more oxidizing than the $AgCl + e^- \leftrightarrow Ag + Cl^-$ half cell. Nevertheless, the potential of electrodes made with 10−20 nm diameter CeO_{2-x} nanoparticles, where ~12% of their $Ce^{3+/4+}$ cations reside at the electrolyte interface, is ~0.21 V (SHE), nearly identical with the potential of the $AgCl + e^- \leftrightarrow Ag + Cl^-$ half-cell in body fluids where $[Cl^-]$ = 0.14 M.

EXPERIMENTAL SECTION

Unless otherwise stated, the potentials are versus that of the Ag/AgCl (3 M KCl) half-cell.

Received: October 19, 2012
Published: November 21, 2012

dx.doi.org/10.1021/ja3103549 | J. Am. Chem. Soc. 2012, 134, 20783−20787

Chemicals and Materials. Ceria nanoparticles: 20 wt %, pH 3.5, 10−20 nm particle size, acetic acid-stabilized colloidal ceria sol was purchased from Nyacol Nano Technologies, Ashland, MA. For experiments requiring acetate-free and partially deoxygenated ceria, the sol was placed in an open Petri dish, where water was allowed to evaporate. The residual powder was heated, increasing its temperature by 10 °C/min to 400 °C, then held at 400 °C for 4 h. For experiments requiring oxygenated ceria: O_2 was passed for 10 min through the ceria sol. Hydrophilic graphitic carbon: Timcal C-45, from Timcal, Westlake, OH, was made hydrophilic by plasma treatment for 10 min in ∼1 Torr air plasma. Poly-*N*-vinylimidazole (PVI) was prepared according to Ohara et al.[7] Poly(ethylene glycol) (*n*) diglycidyl ether (PEGDGE) catalog number 08211-100 was purchased from Polysciences, Inc., Warrington, PA.

Equipment. A plasma cleaner of Harrick Plasma, Ithaca, NY, was used for plasma treatment of the carbon, and a Perkin-Elmer TGA-7 was used for the thermogravimetric analysis. The electrochemical experiments were performed with a Model 832, CHI (Austin, TX), potentiostat in a 3-electrode electrochemical cell with a 3 or 2 mm diameter vitreous carbon working electrode, a Ag/AgCl (3 M KCl) reference electrode, and a platinum wire or carbon rod counter electrode. When the electrodes were rotated, a Pine Instrument rotator was used.

Electrode Coatings without Carbon Particles. The ceria sol (1 mL) was diluted with 19 mL of deionized water. The diluted sol (2 mL) was mixed with 0.2 mL of 1 wt % aqueous PVI and with 2 μL (undiluted) PEGDGE. Two μL of the mixture was applied to the 3 mm diameter vitreous carbon electrodes. The resulting film was cured overnight in ambient air and temperature.

Electrode Coatings with Carbon Particles. The calcined ceria nanoparticles (200 mg) were mixed with 100 mg of the plasma-treated hydrophilic graphitic carbon nanoparticles and dry-ground in an agate mortar, then 2 mL water was added, and the paste was reground for 10 min. The paste (1.5 mL) was mixed with 1.5 mL of the 1 wt % aqueous PVI, sonicated for 20 min, and then mixed with 3 mL of water containing 4 μL PEGDGE. Vitreous carbon electrodes of 3 mm diameter were coated with 2 μL of the resulting paste, and the films were cured overnight at ambient temperature. The same composition was used when films resisting a high stress were required for the 300−1000 rpm rotating disk experiments, except that 1 mL of the paste was mixed with 1 mL of 1 wt % PVI and 2 μL PEGDGE. For the experiments in phosphate buffer a mixture of 1.0 mL of DI water, 150 mg of the hydrophilic carbon, and 1 mL of oxygenated ceria sol was ground in an agate mortar for 20 min, and then 1.5 mL of the paste was mixed with 1.5 mL of 1 wt % aqueous PVI, sonicated for 20 min, and mixed with 3 mL of water containing 4 μL PEGDGE. Vitreous carbon electrodes of 3 mm diameter were coated by 2 μL droplets of the resulting paste and cured overnight at room temperature.

Glucose Sensors. The sensors were similar to those described by Feldman et al.[5] Printed carbon or sputtered gold traces formed the conducting bases of the electrodes. The working electrode contained cross-linked glucose oxidase and redox polymer, overcoated with a glucose flux-limiting membrane. The current was monitored with a custom-built potentiostat at an applied potential of 40 mV versus the reference electrode.

RESULTS AND DISCUSSION

The Raman spectrum of the dried ceria nanoparticles (Figure S1) showed a sharp, dominant 464 cm^{-1} band, associated with the symmetrical stretching mode of the [Ce−O8] vibrational unit in the bulk of the fluorite-phase crystallites, where the oxide anions proximal to the cerium cations vibrated symmetrically.[8] The proximal diffuse satellite bands are attributed to surface Ce−O stretching vibrations. The ESR spectrum of the dried ceria nanoparticles (Figure S2) showed an intense peak with a *g*-value of 2.036 at room temperature, consistent with the 2.039 *g*-value attributed to Ce^{3+}.[9] The peaks of the X-ray diffraction pattern of the dried ceria nanoparticles (Figure S3) matched those of fluorite-phase ceria. Their broadening, i.e., full-width at half-maximum, was consistent according to the Scherrer equation with the expected broadening for 5−10 nm diameter crystallites,[8] smaller than the nominal 10−20 nm particle size, implying that the nanoparticles were aggregates of smaller crystallites.

Figure 1 shows the voltammogram of a film made with a sol of 10−20 nm CeO_{2-x} particles immobilized in PEGDGE cross-linked PVI. When applied to 3 mm vitreous carbon disks, the film withstood the shear stress resulting of rotation at 1000 rpm. The redox potential of the immobilized nanoparticles was 0.07 V vs Ag/AgCl (3 M KCl), nearly identical with the redox potential of Ag/AgCl in a physiological saline solution, where the Cl^- concentration is about 20 times lower than in 3 M KCl. When only a minute current was drawn of the reference electrode, this simple but resistive film sufficed. For applications requiring greater current, the resistance of the films was reduced by incorporating hydrophilic graphitic carbon particles. Their incorporation increases the current density about 50-fold without substantially altering the redox potential. In the experiment of Figure 2, where the CeO_{2-x} nanoparticles were deoxygenated by heating to 400 °C, the redox potential under N_2 was 60 mV versus Ag/AgCl (3 M KCl), i.e., about 10 mV versus Ag/AgCl in physiological saline buffer; under air it downshifted but only by 40 mV, and under O_2 it downshifted

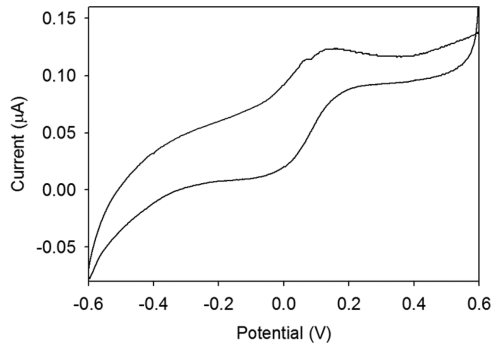

Figure 1. Cyclic voltammogram of a 3 mm diameter vitreous carbon electrode coated with a film of ceria nanoparticles immobilized in PEGDGE cross-linked PVI; pH 7, 20 mM imidazole−HCl buffer; under N_2; 1 mV/s scan rate.

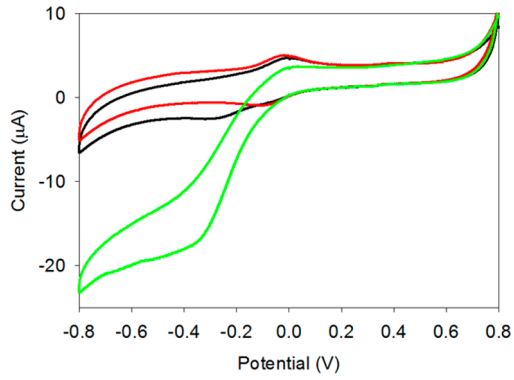

Figure 2. Cyclic voltammograms of a 3 mm vitreous carbon electrode coated with a film made of partially deoxygenated ceria nanoparticles, hydrophilic carbon particles, and PEGDGE cross-linked PVI under N_2 (red), air (black), and O_2 (green); pH 7 imidazole−HCl buffer; 5 mV/s scan rate.

dx.doi.org/10.1021/ja3103549 | J. Am. Chem. Soc. 2012, 134, 20783−20787

by 90 mV. As expected for the $Ce_{nps}^{4+} + e^- \leftrightarrow Ce_{nps}^{3+}$ couple (nps referring to interfacial cerium cations), the potential under N_2 was pH independent. Because $Ce_{nps}^{4+}(OOH)$ is formed by reaction of Ce^{3+} with O_2 followed by protonation according to $Ce_{nps}^{3+} + O_2 + H^+ \rightarrow Ce_{nps}^{4+}(OOH)$,[10−12] under O_2 the potential depended on pH, consistently with the half-cell reaction $Ce_{nps}^{4+}(OOH) + e^- + H^+ \leftrightarrow Ce_{nps}^{4+} + H_2O_2$. In air the pH dependence was, however, slight (Figure 2).

Figures 3 and 4 show that the potential of the $Ce_{nps}^{4+} + e^- \leftrightarrow Ce_{nps}^{3+}$ half-cell does not change between pH 4 and 8 and

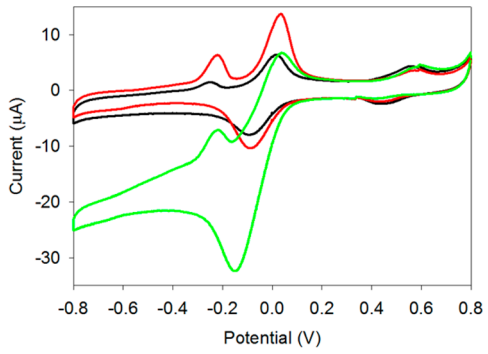

Figure 3. Cyclic voltammograms of a 3 mm vitreous carbon electrode coated with a film made of partially deoxygenated ceria nanoparticles, carbon, and PEGDGE cross-linked PVI under N_2 (red), air (black), and O_2 (green); pH 4 citrate buffer; 5 mV/s scan rate.

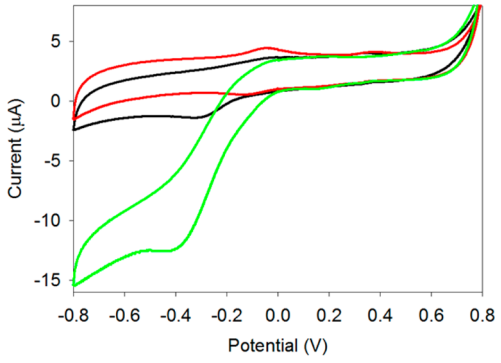

Figure 4. Cyclic voltammograms of a 3 mm vitreous carbon electrode coated with a film made of partially deoxygenated ceria nanoparticles, carbon, and PEGDGE cross-linked PVI under N_2 (red), air (black), and O_2 (green); pH 8 imidazole−HCl buffer; 5 mV/s scan rate.

that the potential of the half-cell $Ce_{nps}^{4+}(OOH) + e^- + H^+ \leftrightarrow Ce_{nps}^{4+} + H_2O_2$ is, as expected, pH dependent. At pH 4, the bound O_2-associated wave is upshifted by −120 mV to −80 mV versus Ag/AgCl (3 M KCl), i.e., to −20 mV versus Ag/AgCl in physiological saline. In the pH 8 buffer the bound O_2-associated wave is downshifted by about −60 mV to −260 mV versus Ag/AgCl (3 M KCl), i.e., to −190 mV versus Ag/AgCl in physiological saline. In the pH 4 solution, which was made with citrate buffer, a minor wave appeared at +0.49 V versus Ag/AgCl (3 M KCl). Cummings et al., who bound positively surface-charged ceria nanocrystallites layer-by-layer with polycarboxylic acids, also observed such a wave,[13] suggesting that the wave is carboxylate associated.

Chemisorption of phosphate onto the ceria nanoparticles slows the electrode reaction, causing separation of the anodic and cathodic waves by as much as 0.27 V at pH 6, 0.30 V at pH 7 and 0.30 V at pH 8. While phosphate chemisorption downshifts the half-cell potential by 0.07 V, it advantageously prevents the reactive binding of O_2, i.e., the reaction associated with the resulting $Ce_{nps}^{4+}(OOH) + e^- + H^+ \leftrightarrow Ce_{nps}^{4+} + H_2O_2$ half-cell. In the presence of 20 mM phosphate the half-cell potential does not change with pH (Figure 5).

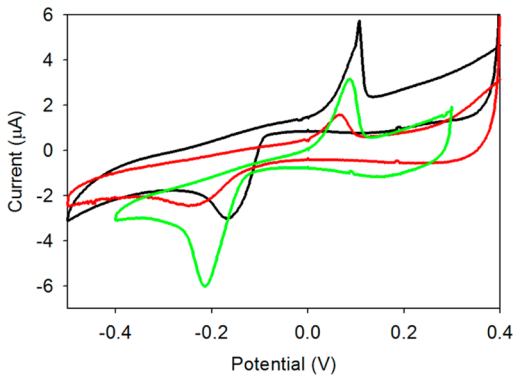

Figure 5. Cyclic voltammograms of a 3 mm diameter vitreous carbon electrode coated with ceria nanoparticles that were not deoxygenated and carbon bound with PEGDGE cross-linked PVI. Air atmosphere; 20 mM phosphate−0.1 M NaCl buffers of pH 6, 7, and 9 (black, green, and red, respectively); 1 mV/s scan rate.

When the ceria nanoparticle−carbon electrode, made with nanoparticles heated to 400 °C and with PEGDGE cross-linked PVI, was rotated in the 20 mM pH 7 phosphate buffer solution under air, the voltammetric wave near the potential of the Ag/AgCl electrode was independent of the angular velocity. The current was angular velocity, i.e., diffusional transport, dependent at potentials negative of −0.25 V vs Ag/AgCl (3 M KCl), the threshold for dissolved O_2 electroreduction. (Figure 6)

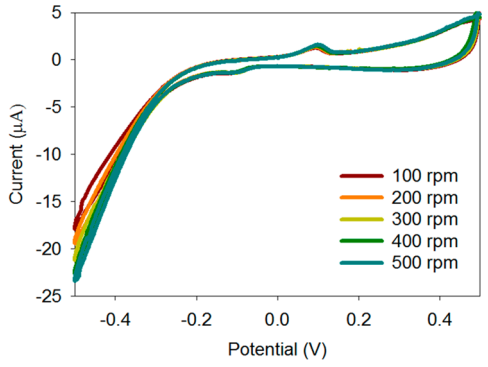

Figure 6. Rotation independence of the voltammetric waves near the Ag/AgCl electrode potential and rotation dependence of dissolved O_2 electroreduction at potentials more reducing than −0.25 V versus Ag/AgCl (3 M KCl); 2 mm diameter vitreous carbon disk coated with a film of ceria nanoparticles, carbon and PEGDGE-crosslinked PVI; air; pH 7 20 mM phosphate buffer; scan rate 5 mV/s.

The *in vitro* calibration curves of glucose sensors, designed for continuous operation upon their subcutaneous implantation,[5] were indistinguishable when made with reference electrodes comprising Ag/AgCl on printed carbon, ceria embedded in PEGDGE cross-linked PVI on printed carbon, or ceria embedded in PEGDGE cross-linked PVI on sputtered gold. This was the case when the sensors operated in air (Figure 7) and when they operated in 2% O_2 (balance: N_2) (Figure 8). Furthermore, the sensitivitiy of a set of 24 sensors

dx.doi.org/10.1021/ja3103549 | J. Am. Chem. Soc. 2012, 134, 20783−20787

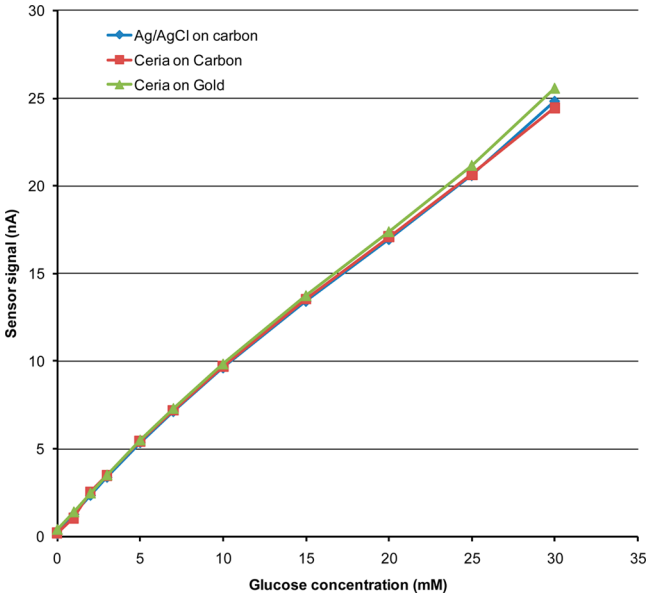

Figure 7. Similarity of *in vitro* calibration curves of amperometric glucose sensors[5] made with Ag/AgCl reference (blue), nanocrystalline CeO_{2-x} on printed carbon (red), and nanocrystalline CeO_{2-x} on sputtered gold (green) reference electrodes under air.

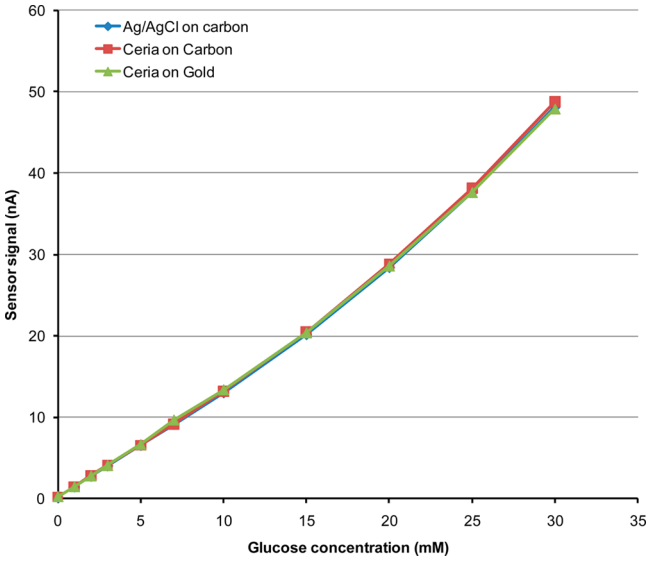

Figure 8. Similarity of *in vitro* calibration curves of amperometric glucose sensors[5] made with Ag/AgCl reference (blue), nanocrystalline CeO_{2-x} on printed carbon (red) and nanocrystalline CeO_{2-x} on sputtered gold reference (green) electrodes under 2% O_2 (balance: N_2).

made with ceria embedded in PEGDGE cross-linked PVI on printed carbon reference electrodes changed by only ~10% after operating continuously at 37 °C in 17 mM glucose under ambient air for 5 days in pH 7, 20 mM phosphate-buffered physiological saline, and their nearly linear response was preserved (Figure 9).

CONCLUSIONS

The dominant half-cell reaction of polymer-embedded ceria nanoparticles is $Ce^{4+} + e^- \leftrightarrow Ce^{3+}$. The redox potential of the half-cell is practically identical with that of the AgCl $+e^- \leftrightarrow Ag + Cl^-$ half-cell in body fluids where $[Cl^-] = 0.14$ M. The potential

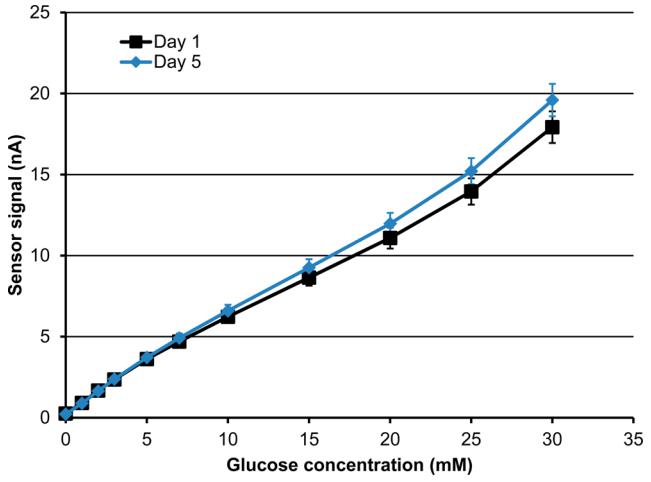

Figure 9. Day 1 (black squares) and day >5 (blue diamonds) calibration curves of amperometric glucose sensors made with ceria nanoparticle on printed carbon reference electrodes. Sensors operated continuously in a 17 mM glucose, pH 7 20 mM phosphate, physiological saline solution at 37 °C under ambient air. Error bars represent standard deviations for the tested set of 24 sensors.

is pH independent in the 4–8 pH range, and in 20 mM phosphate, it is O_2 pressure independent. Lower cost ceria nanoparticle reference electrodes could replace Ag/AgCl electrodes in mass produced strips and in subcutaneously implanted electrochemical glucose sensors.

ASSOCIATED CONTENT

Supporting Information

Raman spectrum, ESR spectrum, X-ray diffraction pattern and weight loss upon heating (thermogravimetric analysis) of the dried ceria nanoparticles. This material is available free of charge via the Internet at http://pubs.acs.org.

AUTHOR INFORMATION

Corresponding Author

heller@che.utexas.edu

Notes

The authors declare the following competing financial interest(s): A.H. consults with Abbott Diabetes Care, a manufacturer of glucose monitoring systems. U.H. is an employee of Abbott Diabetes Care.

ACKNOWLEDGMENTS

We thank Keith A. Friedman the thermal analyses. R.K.N. thanks the DST of India for the Ramanujan Fellowship (SR/S2/RJN-18/2011) award.

REFERENCES

(1) In *Bioshares*; Blake Industry and Market Analysis: Richmond, Victoria, Australia, 2012; Vol. *445*, p 3.

(2) Hill, H. A. O.; Higgins, I. J.; McCann, J. M.; Davis, G. Strip Electrode including screen printing of a single layer, U.S. Patent 5,509,410, April 23, 1996.

(3) Forrow, N. J.; Bayliff, S. W.; Electrode with thin working layer. U.S. Patent 6,764,581, July 20, 2004.

(4) Huang, C.-M.; Structure and manufacturing method of disposable electrochemical sensor strip. U.S. Patent 7,063,776, June 20,2006.

(5) Feldman, B.; Brazg, R.; Schwartz, S.; Weinstein, R. *Diabetes Technol. Ther.* **2003**, *5*, 769.

(6) *Abundance of Elements in Earth's Crust*; Wikipedia, Wikimedia Foundation: San Francisco, CA, 2012; http://en.wikipedia.org/wiki/Abundance_of_elements_in_Earth's_crust (accessed October 16, 2012).
(7) Ohara, T. J.; Rajagopalan, R.; Heller, A. *Anal. Chem.* **1993**, *65*, 3512.
(8) Saitzek, S.; Blach, J. F.; Villain, S.; Gavarri, J. R. *Phys. Status Solidi A* **2008**, *205*, 1534.
(9) Quintanar, C.; Caballero, R.; Barreto, J.; Chavira, E.; Marinero, E. E. *Int. J. Quantum Chem.* **2010**, *110*, 2949.
(10) Li, C.; Domen, K.; Maruya, K.; Onishi, T. *J. Am. Chem. Soc.* **1989**, *111*, 7683.
(11) Zhang, X.; Klabunde, K. J. *Inorg. Chem.* **1992**, *31*, 1706.
(12) Soria, J.; Martinez-Arias, A.; Conesa, J. C. *J. Chem. Soc., Faraday Trans.* **1995**, *91*, 1669.
(13) Cummings, C. Y.; Stott, S. J.; Bonne, M. J.; Edler, K. J.; King, P. M.; Mortimer, R. J.; Marken, F. *J. Solid State Electrochem.* **2008**, *12*, 1541.